

## Chiral Bands with Rigid Quasiparticle Alignments

R. Budaca<sup>1,2</sup>

<sup>1</sup>“Horia Hulubei” National Institute for Physics and Nuclear Engineering,  
Str. Reactorului 30, RO-077125, POB-MG6 Bucharest-Măgurele, Romania

<sup>2</sup>Academy of Romanian Scientists, 54 Splaiul Independenței, RO-050094,  
Bucharest, Romania

Received 11 November 2019

**Abstract.** A triaxial particle-rotor Hamiltonian describing a system of two high- $j$  quasiparticles rigidly aligned to a triaxial collective core, is treated semiclassically within a time-dependent variational principle. Quantizing the energy function for a given angular momentum, one obtains a Schrödinger equation with a coordinate dependent effective mass for a chiral potential. The applicability of the formalism is discussed in terms of varying triaxial deformation and more general quasiparticle spin alignments. The model is exemplified by describing the partner bands in  $^{134}\text{Pr}$  using the corresponding spectrum and wave-functions obtained for valence  $h_{11/2}$  proton particle and  $h_{11/2}$  neutron hole. Some perspectives of the model are also briefly discussed.

KEY WORDS: Chiral bands, Semiclassical description, Quasiparticles, Nuclear rotations.

### 1 Introduction

Frauendorf and Meng [1] were the first to theoretically discuss the possible occurrence of geometric chirality or handedness in a nuclear system composed of a triaxial core coupled to a set of high- $j$  valence particles and holes. The basic idea is that the three spins associated to the core, particles and holes, can be arranged to form two systems with opposite intrinsic chirality defined by their screw direction in respect to the total angular momentum vector. For such an arrangement to be realized, a few conditions must be met simultaneously. First of all one must recall that a triaxial rigid body favors rotations around the intrinsic principal axis with the maximal moment of inertia, which usually corresponds to the medium semi-axis of the triaxial shape of the nucleus. In what concerns the coupling of the quasiparticles, the microscopic calculations showed that a particle aligns to the short axis, a hole to the long axis, while a quasiparticle

from the vicinity of the Fermi surface tends to align along the medium axis as the rotation of the triaxial core [2]. Therefore, a system of one particle and one hole coupled to a triaxial core can accommodate a chiral geometry. Although, in the intrinsic frame, the chiral symmetry is spontaneously broken, it is restored in the laboratory frame of reference, where the observation of a nearly degenerate doublet of  $\Delta I = 1$  bands with the same parity is expected [3]. Bands exhibiting chiral properties were shortly identified in few  $N = 75$  odd-odd isotones [4], where the quasiparticle configuration is of one proton particle and one neutron hole from the  $h_{11/2}$  orbital. The experimental observation of this phenomenon spread in more nuclei around  $A \sim 130$ . Later on, other mass regions with  $A \sim 80, 100$  and  $190$ , offered experimental evidence of partner bands based on different quasiparticle configurations [5–7]. The theoretical and experimental studies of nuclear chirality lead to its extension also to odd mass or even-even nuclei and to the occurrence of multiple chirality within a single nucleus [8]. However, with the flood of experimental data, it became clear that the envisaged chiral geometry is an idealistic picture which is not realized in actual nuclei, where the observed partner bands are only approximately degenerated in limited high spin ranges. The most obvious mechanisms responsible for the lifting of the bands' degeneracy are related to the low rigid triaxiality of the nuclear shape, which is still rarely encountered in nuclei, and to the deviations in the single particle alignments due to non-rigid coupling or their hindered particle and hole characters. In this paper, one will briefly discuss the implications of these effects in connection to a semiclassical description of a system composed of two quasiparticles and a triaxial core.

## 2 Chiral Classical Dynamics and Quantum Hamiltonian

The most adequate tool for the study of the interaction between two quasiparticle angular momenta and a collective one is an extension of the particle-rotor Hamiltonian [9],

$$H_{PR} = \sum_{k=1}^3 A_k \left( \hat{I}_k - \hat{j}_k - \hat{j}'_k \right)^2 + H_{sp}, \quad (1)$$

where  $A_k = 1/(2\mathcal{J}_k)$  are inertial parameters along the principal axes of the intrinsic frame of reference with  $\mathcal{J}_k$  being the corresponding moments of inertia (MOI) considered here in the hydrodynamic estimation [9]:

$$\mathcal{J}_k = \frac{4}{3} \mathcal{J}_0 \sin^2 \left( \gamma - \frac{2}{3} k\pi \right) \quad (2)$$

related to the measure of the deviation from axial symmetry,  $\gamma$ .  $\hat{I}_k$ ,  $\hat{j}_k$  and  $\hat{j}'_k$  are the operators of the total, and quasiparticle angular momentum projections

### Chiral Bands with Rigid Quasiparticle Alignments

on the same axes. Consider now that the two quasiparticle spins are rigidly aligned along the principal planes 1-3 and 2-3:

$$\begin{aligned}\hat{j}_1 &= j \cos \alpha, \hat{j}'_1 = 0, \\ \hat{j}_2 &= 0, \hat{j}'_2 = j' \cos \alpha' = 0, \\ \hat{j}_3 &= j \sin \alpha, \hat{j}'_3 = j' \sin \alpha'.\end{aligned}\quad (3)$$

The rigid or frozen alignment approximation corresponds to the situation where the operators of the quasiparticle spin components are simply replaced by real numbers. This is a strong approximation, and one don't expect it to be valid along the whole range of total angular momentum values. Nevertheless, the unconstrained particle-rotor calculations sustains it over a large range of angular momentum states for low triaxial deformation, while for strong triaxiality its validity is limited to low and moderate spins [10].

The tilting angles  $\alpha(\alpha')$  give the measure of the quasiparticles' nature. Higher tilting towards the medium axis means that the aligned quasiparticle is closer to the Fermi level.

Extracting the constant quasiparticle contribution  $H_{qp} + H'_{qp}$ , one remains with the reduced Hamiltonian

$$\begin{aligned}H_{\text{chiral}} &= A_1 \hat{I}_1^2 + A_2 \hat{I}_2^2 + A_3 \hat{I}_3^2 - 2A_1 j \cos \alpha \hat{I}_1 \\ &\quad - 2A_2 j' \cos \alpha' \hat{I}_2 - 2A_3 (j \sin \alpha + j' \sin \alpha') \hat{I}_3,\end{aligned}\quad (4)$$

which is relevant for the system's dynamics. The later can be extracted by describing the quantum system in terms of some classical observables. This is realized by associating a time-dependent variational principle for the Hamiltonian (4):

$$\delta \int_0^t \langle \psi(x, \varphi) | H_{\text{chiral}} - \frac{\partial}{\partial t'} | \psi(x, \varphi) \rangle dt' = 0, \quad (5)$$

where the variational state is a coherent state for the  $SU(2)$  algebra of the angular momentum operators [12]

$$\begin{aligned}|\psi(x, \varphi)\rangle &= \sum_{K=-I}^I \frac{1}{(2I)^I} \sqrt{\frac{(2I)!}{(I-K)!(I+K)!}} \\ &\quad \times (I+x)^{\frac{I-K}{2}} (I-x)^{\frac{I+K}{2}} e^{i\varphi(I+K)} |IMK\rangle.\end{aligned}\quad (6)$$

Here,  $|IMK\rangle$  is the eigenfunction of the total angular momentum operator, and its projections on the third intrinsic ( $K$ ) and laboratory ( $M$ ) principal axis. Besides defining the variational state, the azimuth angle  $0 \leq \varphi < 2\pi$  of the total angular momentum vector direction and its projection on the third intrinsic axis  $x = I \cos \theta$  expressed in terms of the polar angle  $0 \leq \theta \leq \pi$  of the same direction, are found to be canonical conjugate variables when the variational

principle is solved. Consequently,  $\varphi$  is identified as the generalized coordinate, while  $x$  plays the role of the generalized momentum. Due to its connection to the projection of the total angular momentum on the third intrinsic axis,  $x$  is also called chiral variable. In terms of these canonical variables, the variational principle produces a pair of equations of motion in a Hamilton canonical form and a classical energy function:

$$\begin{aligned} \mathcal{H}(x, \varphi) = & \frac{I}{2}(A_1 + A_2) + A_3 I^2 \\ & + \frac{(2I - 1)(I^2 - x^2)}{2I}(A_1 \cos^2 \varphi + A_2 \sin^2 \varphi - A_3) \\ & - 2\sqrt{I^2 - x^2}(A_1 j \cos \varphi \cos \alpha + A_2 j' \sin \varphi \cos \alpha') \\ & - 2A_3 x(j \sin \alpha + j' \sin \alpha'). \end{aligned} \quad (7)$$

A thorough description of the rotational dynamics based on the classical energy function and the equations of motion can be obtained by studying the evolution of the critical points of the classical energy as a function of the total angular momentum and the triaxial deformation. The critical points which minimize the classical energy function are associated to the most probable orientations of the total angular momentum vector defined by the  $(\varphi, x)$  coordinates of the minimum point. The change of these directional variables with the total angular momentum offers the alignment of the rotation axis in each instance of the system's motion. An analysis in this sense was performed in Ref. [12], where it was found that the classical energy function exhibits two minima in respect to the chiral variable  $x$ , starting with a certain critical value of the total angular momentum. The effect of the triaxial deformation on the critical value angular momentum is expressed through an increase of this value whenever the triaxial deformation is changed towards more axially symmetric shapes [12, 13]. The two stationary points which emerge after the critical angular momentum, correspond to the geometrical configurations with different handedness or chirality. The system's dynamical description can be also complemented by investigating the evolution in the stationary points of the classical components of total angular momentum determined as averages of the corresponding operators on the coherent state (6):

$$\begin{aligned} \mathcal{I}_1 &= \sqrt{I^2 - x^2} \cos \varphi, \\ \mathcal{I}_2 &= \sqrt{I^2 - x^2} \sin \varphi, \\ \mathcal{I}_3 &= x. \end{aligned} \quad (8)$$

In order to extract some measurable observables from this classical picture, one must quantize the classical energy function. Speculating the fact that the global minima of the energy function have always a single value for variable  $\varphi$ , one

### Chiral Bands with Rigid Quasiparticle Alignments

firstly expands it around the corresponding minimum points  $\varphi_0(x)$  for fixed values of  $x$ :

$$\tilde{\mathcal{H}}(x, \varphi) \approx \mathcal{H}(x, \varphi_0(x)) + \frac{1}{2} \left( \frac{\partial^2 \mathcal{H}}{\partial \varphi^2} \right)_{\varphi_0(x)} [\varphi - \varphi_0(x)]^2. \quad (9)$$

With such an approximation, the classical energy function becomes quadratic in generalized momenta, making thus easier its transformation to a Schrödinger-like equation:

$$\left[ -\frac{1}{2} \frac{1}{\sqrt{B(x)}} \frac{d}{dx} \frac{1}{\sqrt{B(x)}} \frac{d}{dx} + V(x) \right] f(x) = E_p f_p(x). \quad (10)$$

Here  $p$  index the solutions in terms of the chiral variable excitation, while

$$B(x) = \left[ \frac{\partial^2 \mathcal{H}(x, \varphi)}{\partial \varphi^2} \right]_{\varphi_0(x)}^{-1} \quad (11)$$

plays the role of an one-dimensional coordinate-dependent effective mass. The potential for the chiral variable is

$$V(x) = \mathcal{H}(x, \varphi_0(x)) + \frac{B''(x)}{8 [B(x)]^2} - \frac{9 [B'(x)]^2}{32 [B(x)]^3}. \quad (12)$$

This result was obtained by imposing the correspondence  $\varphi = i \frac{d}{dx}$  in the symmetrically ordered classical function (9) followed by a suitable change of function. The final function  $f(x)$  is normalized accordingly:

$$\int_{-I}^I |f(x)|^2 \sqrt{B(x)} dx = 1. \quad (13)$$

The resulting quantum problem is at first glance similar with the one-dimensional collective Hamiltonian obtained in [14]. Note however that the present quantum Hamiltonian is obtained consistently just from the rotational geometry of the system, rather than from microscopic input, where the polar angle and the chiral variable are no longer connected by their canonical conjugate relationship.

The consistency of the harmonic approximation on the energy function which is quadratic in angular momentum components can be checked by calculating the commutators between similarly quantized first order expansions of the classical components (8). A simple calculation will recover the commutation relations associated to the operators of the intrinsic angular momentum components, which differ from the usual ones by a sign of one of the components.

The eigenvalue problem (10) is by construction bounded by  $|x| \leq I$ , and therefore one can employ particle in the box eigenstates for the diagonalization basis.

The coefficients of the basis expansion are obtained from the diagonalization of the Schrödinger equation (10). The chiral vibration can now be coupled to the rotational excitations by weighting the coherent state in  $\varphi_0(x)$  with the density probability of chiral variable

$$\rho_p^I(x) = |f_p(x)|^2 \sqrt{B(x)}. \quad (14)$$

The total wave function is then expressed as [12]:

$$|IMp\rangle = \mathcal{N}_{Ip} \int_{-I}^I \rho_p^I(x) |\psi(x, \phi_0(x))\rangle, \quad (15)$$

and ready to be used for calculating transition probabilities.

### 3 Numerical Application

Let us investigate firstly the domain of application for the formalism presented in the preceding section. Depending on the model's input, gathering single-particle spins  $j$  and  $j'$ , alignment angles  $\alpha$  and  $\alpha'$  and the triaxial deformation  $\gamma$ , one can in principle describe a variety of behaviors for the partner bands and their associated dynamical phenomenology. The quasiparticle spins are provided by the observed configurations of the partner bands, and therefore are fixed for a certain nucleus. On the other hand, the alignment angles and the triaxial deformation must be considered as free parameters and fitted accordingly to experimental data. When  $\alpha = \alpha' = 0$ , the average geometrical configuration of the three spins acquires a chiral symmetry which is reflected in a parity invariance of the analytical formalism in respect to the chiral variable. In this case, the diagonalization of (10) can be performed separately for even and odd parity states. Another symmetry property is obtained from considering  $j = j'$  together with  $\alpha = \alpha' = 0$ , consisting in an equivalence between the prolate and oblate branches of the triaxial deformation  $\gamma$ . As it happens, most of the partner bands suspected of chiral symmetry are reported in the  $A \sim 130$  mass region and are constructed on a  $\pi h_{11/2} \nu h_{11/2}^{-1}$  configuration. While for  $\gamma = 90^\circ$ , the same conditions lead to a constant  $x$ -independent value of the  $\varphi_0$ . Due to the major analytical reduction of the involved calculation effort, this instance of the model was firstly applied on actual experimental data [12]. The  $^{134}\text{Pr}$  nucleus was chosen as a test example, where although the observed partner bands intersect each other at some angular momentum, they were identified with theoretical yrast and yrare bands. Here one will look at the same experimental data from another point of view, concentrating specifically on the energy difference between the same angular momentum states of the partner bands. Therefore, regardless of the experimental band assignment, the yrast and yrare experimental states observed in  $^{134}\text{Pr}$  are fitted with theoretical ground and first excited states of the chiral Hamiltonian against the variation of a common tilting angle  $\alpha = \alpha'$  with

### Chiral Bands with Rigid Quasiparticle Alignments

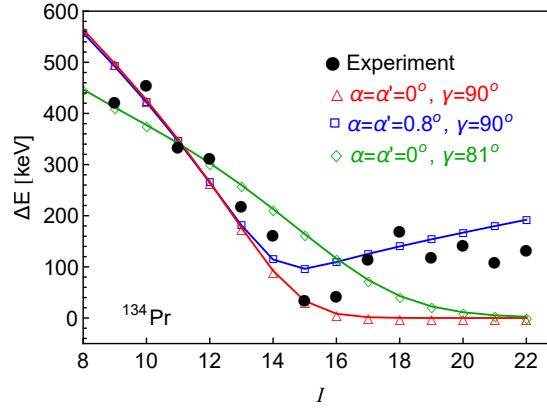


Figure 1. Experimental energy differences between the yrast and non-yrast states of the partner bands of  $^{134}\text{Pr}$  [15] are compared with various model fits and the model calculation with predefined chiral geometry and maximal triaxiality.

fixed  $\gamma = 90^\circ$  triaxiality, and alternatively with fixed alignments  $\alpha = \alpha' = 0$  and the triaxiality measure  $\gamma$  as free parameter. The results are shown in Figure 1 and compared with the simple calculation with predefined  $\alpha = \alpha' = 0$  and  $\gamma = 90^\circ$ . As can be seen graphically but also judging from the standard deviation 40.2 keV for fitted  $\alpha = \alpha' = 0.8^\circ$  with  $\mathcal{J}_0 = 27.3 \text{ MeV}^{-1}$ , 87.3 keV for fitted  $\gamma = 81^\circ$  with  $\mathcal{J}_0 = 37.5 \text{ MeV}^{-1}$ , and 87.4 keV for the formalism of Ref. [12] with  $\mathcal{J}_0 = 26.9 \text{ MeV}^{-1}$ , there is an improvement of the accordance with experiment in both cases comparing with the generic result for the principal axes alignments and maximal triaxiality. The best agreement is obtained when the tilting angle of the single-particle spins towards the third intrinsic axis is varied. It is natural to expect that a combined fit against both  $\alpha$  and  $\alpha'$  together with the triaxial deformation  $\gamma$  would further improve the agreement with experiment. Despite the allure of such a complete calculation, the computational effort is presently very demanding.

Although the obtained tilting angle variation is small, it has drastic repercussions on the model results. Firstly, the chiral symmetry becomes broken even in the laboratory frame of reference. This triggers the existence of a favored trihedral geometry of the three involved vectors. The conclusions drawn from the dynamical description of the chiral bands are still valid for small tilting angles. Namely, for low angular momentum, the system performs a chiral-like vibration from one octant to the other, however no longer symmetric in respect to the chiral variable. The things change after a critical angular momentum, when the two minima in the  $x$  variable of the chiral potential become deeper with increasingly blocked tunneling between them. Whereas in the chiral symmetry case, the probability distribution of the ground and excited states splits evenly between the

two potential wells associated to right-handed and left-handed configurations, in the asymmetric case, this symmetry is broken such that the ground state will be completely localized in the deepest well, while the excited state in the other potential well. This behaviour is valid only for low tilting angles. Indeed, for higher contributions to the third component of the quasiparticle spins, the chiral potential will present at high spins two minima of very disparate depths, such that it is possible to have an excited state also trapped in the same deepest well as the ground state. This type of excitation is very similar to what happens in case of the wobbling motion, which is another trademark phenomenon associated to rigid triaxiality. It is then expected that the model can be used to describe a transition from a chiral-like vibration to a wobbling-like one if a sufficient tilting of the quasiparticle spins towards the core rotation axis is considered.

#### 4 Conclusions and Perspectives

A general Schrödinger equation in a chiral variable is obtained from a semi-classical description of a system with two quasiparticles rigidly aligned to a collective core of an arbitrary triaxial deformation. The coordinate-dependent effective mass and the chiral potential depend on the total angular momentum and parametrically on the triaxial deformation and the quasiparticle alignments. The effect of the both parametrical variations is exemplified on the partner bands measured in the  $^{134}\text{Pr}$  nucleus. It is found that the adjustment of the quasiparticle alignments provide a greater improvement of the agreement with experiment.

Before closing, it is worth to mention few ongoing applications of the model and its future perspectives. First of all, the model can also be successfully applied to the study of the wobbling excitations in odd mass nuclei. At this point only a full harmonic approximation in both chiral variable and the azimuth angle was used to determine compact expressions for the wobbling frequency and their domain of validity within well defined wobbling phases. The use of the present formalism will allow us to go beyond the harmonic approximation with a more realistic wobbling potential. Moreover, as was mentioned before, the general formalism presented here is especially suited to define and describe a transition from chiral to wobbling vibration. Finally, the analytical formalism is at this point well established and extensive quantitative calculations can be pursued. Among possible improvements aimed at a better reproduction of data, one can nominate the introduction of a spin-spin term  $\vec{I} \cdot \vec{j}$  simulating the Coriolis interaction, which is important for high spin states [16, 17].

#### Acknowledgments

This work was supported by a grant from Ministry of Research and Innovation, CNCS - UEFISCDI, project number PN-III-P1-1.1-TE-2016-0268, within PNCDI III.

## References

- [1] S. Frauendorf, J. Meng (1997) Tilted rotation of triaxial nuclei. *Nucl. Phys. A* **617** 131-147 DOI: [https://doi.org/10.1016/S0375-9474\(97\)00004-3](https://doi.org/10.1016/S0375-9474(97)00004-3).
- [2] S. Frauendorf, F. Dönau (2014) Transverse wobbling: A collective mode in odd-*A* triaxial nuclei. *Phys. Rev. C* **89** 014322 DOI: <https://doi.org/10.1103/PhysRevC.89.014322>.
- [3] S. Frauendorf (2001) Spontaneous symmetry breaking in rotating nuclei. *Rev. Mod. Phys.* **73** 463 DOI: <https://doi.org/10.1103/RevModPhys.73.463>.
- [4] K. Starosta *et al.* (2001) Chiral doublet structures in odd-odd  $N = 75$  isotones: chiral vibrations. *Phys. Rev. Lett.* **86** 971 DOI: <https://doi.org/10.1103/PhysRevLett.86.971>.
- [5] R.A. Bark *et al.* (2014) Studies of chirality in the mass 80, 100 and 190 regions. *Int. J. Mod. Phys. E* **23** 1461001 DOI: <https://doi.org/10.1142/S0218301314610011>.
- [6] K. Starosta, T. Koike (2017) Nuclear chirality, a model and the data. *Phys. Scr.* **92** 093002 DOI: <https://doi.org/10.1088/1402-4896/aa800e>.
- [7] B.W. Xiong, Y.Y. Wang (2019) Nuclear chiral doublet bands data tables. *At. Data Nucl. Data Tables* **125** 193-225 DOI: <https://doi.org/10.1016/j.adt.2018.05.002>.
- [8] J. Meng, J. Peng, S.Q. Zhang, S.-G. Zhou (2006) Possible existence of multiple chiral doublets in  $^{106}\text{Rh}$ . *Phys. Rev. C* **73** 037303 DOI: <https://doi.org/10.1103/PhysRevC.73.037303>.
- [9] A. Bohr, B.R. Mottelson (1975) “*Nuclear Structure*”, Vol. II. Benjamin-Cummings, Reading, MA.
- [10] Q.B. Chen, N. Kaiser, Ulf-G. Meißner, J. Meng (2019) Behavior of the collective rotor in nuclear chiral motion. *Phys. Rev. C* **99** 064326 DOI: <https://doi.org/10.1103/PhysRevC.99.064326>.
- [11] R. Budaca (2018) Tilted-axis wobbling in odd-mass nuclei. *Phys. Rev. C* **97** 024302 DOI: <https://doi.org/10.1103/PhysRevC.97.024302>.
- [12] R. Budaca (2018) Semiclassical description of chiral geometry in triaxial nuclei. *Phys. Rev. C* **98** 014303 DOI: <https://doi.org/10.1103/PhysRevC.98.014303>.
- [13] R. Budaca (2019) Role of triaxiality in the structure of chiral partner bands. *Phys. Lett. B* **797** 014303 DOI: <https://doi.org/10.1016/j.physletb.2019.134853>.
- [14] Q.B. Chen, S.Q. Zhang, P.W. Zhao, R.V. Jolos, J. Meng (2013) Collective Hamiltonian for chiral modes. *Phys. Rev. C* **87** 024314 DOI: <https://doi.org/10.1103/PhysRevC.87.024314>.
- [15] D. Tonev *et al.* (2007) Question of dynamic chirality in nuclei: The case of  $^{134}\text{Pr}$ . *Phys. Rev. C* **76** 044313 DOI: <https://doi.org/10.1103/PhysRevC.76.044313>.
- [16] A.A. Raduta, R. Budaca (2011) Semimicroscopic description of backbending phenomena in some deformed even-even nuclei. *Phys. Rev. C* **84** 044323 DOI: <https://doi.org/10.1103/PhysRevC.84.044323>.
- [17] R. Budaca, A.A. Raduta (2013) Semi-microscopic description of the double backbending in some deformed even-even rare earth nuclei. *J. Phys. G: Nucl. Part. Phys.* **40** 025109 DOI: <https://doi.org/10.1088/0954-3899/40/2/025109>.